

On stabilized $P1$ finite element approximation for time harmonic Maxwell's equations

M. Asadzadeh* and L. Beilina*

Abstract

One way of improving the behavior of finite element schemes for classical, time-dependent Maxwell's equations, is to render them from their hyperbolic character to elliptic form. This paper is devoted to the study of the stabilized linear finite element method for the time harmonic Maxwell's equations in a dual form obtained through the Laplace transformation in time. The model problem is for the particular case of the dielectric permittivity function which is assumed to be constant in a boundary neighborhood. For the stabilized model a coercivity relation is derived that guarantee's the existence of a unique solution for the discrete problem. The convergence is addressed both in *a priori* and *a posteriori* settings. In the *a priori* error estimates we confirm the theoretical convergence of the scheme in a L_2 -based, gradient dependent, triple norm. The order of convergence is $\mathcal{O}(h)$ in weighted Sobolev space $H_w^2(\Omega)$, and hence optimal. Here, $w = w(\varepsilon, s)$ where ε is the dielectric permittivity function and s is the Laplace transformations variable. We also derive, similar, optimal *a posteriori* error estimates controlled by a certain, weighted, norm of the residual of the computed solution. The *a posteriori* approach is used for constructing adaptive algorithms for the computational purposes. Further, assuming a sufficiently regular solution for the dual problem, we reach the same convergence of $\mathcal{O}(h)$. Finally, through implementing several numerical examples, we validate the robustness of the proposed scheme.

1 Introduction

By the growing efficiency of the recent computing facilities, the development of efficient computational methods for simulation of partial differential equations in two and three-dimensions, in particular when the computational domains are very large, which are of vital interest, has become achievable. It is very typical that in industrial applications computational domains often comprise very large subdomains with constant values of material

*Department of Mathematical Sciences, Chalmers University of Technology and University of Gothenburg, SE-42196 Gothenburg, Sweden, e-mail: e-mail:mohammad@chalmers.se, e-mail:larisa@chalmers.se

parameters. Usually, only some part of these domains where there is an over-admissible material change presents extra caution and therefore is of interest. In such cases the problem is described by a model equation with the constant material parameters in a boundary neighborhood of the computational domain. Some applications of the Maxwell's models, describing the electro-magnetic fields, fit into this category.

It is well known that for the stable implementations of the finite element solution for the Maxwell's equations, divergence-free edge elements are the most satisfactory choice from a theoretical point of view [25, 28]. However, the edge elements are less attractive for solution of time-dependent problems since a linear system of equations should be solved at every time iteration, a procedure requiring an unrealistic degree of time resolution, and hence expensive from the programming point of view.

In contrary, continuous P1 finite elements provide both reliable and efficient (inexpensive) way for numerical simulations, in particular compared to $H(\text{curl})$ conforming methods. They can be efficiently used in a fully explicit finite element scheme with lumped mass matrix [15, 21]. However, P1 elements applied to the solution of Maxwell's equations have a number of drawbacks, e.g., in problems with re-entered corners and non-zero tangential components at the boundary, they result in a spurious oscillatory solutions [26, 29]. There are a number of techniques which remove such oscillatory solutions from the numerical approximations of Maxwell's equations, see for example [18, 19, 20, 27, 29].

We circumvent these difficulties considering convex computational domains with constant values of parameters in a boundary neighborhood. More specifically, in this work we consider stabilized P1 finite element method for the numerical solution of time harmonic Maxwell's equations for the special case when the dielectric permittivity function has a constant value in a boundary neighborhood. In this way the Maxwell's equations are transformed to a set of time-independent wave equations on the boundary neighborhood. Thus, several type of adequate boundary conditions for these equations might be handled by P1 finite elements.

Recently, stability and consistency of the stabilized P1 finite element method for time-dependent Maxwell's equations was presented in [4]. Efficiency in usage of an explicit P1 finite element scheme is evident for solution of *Coefficient Inverse Problems* (CIPs). In many algorithms which solve electromagnetic CIPs a qualitative collection of experimental data (measurements) is necessary at the boundary of the computational domain to determine the dielectric permittivity function inside it. In this case the numerical solution of time-dependent Maxwell's equations are required in the entire space \mathbb{R}^3 , see for example [5, 6, 7, 10, 32, 33], and it is efficient to consider Maxwell's equations with constant dielectric permittivity function in a neighborhood of the boundary of the computational domain. An explicit P1 finite element scheme in non-conductive media is numerically tested for solution of time-dependent Maxwell's system both in 2D and 3D cases in [2]. The P1 finite element scheme of [2] is used for solution of different CIPs to determine the dielectric permittivity function in non-conductive media for time-dependent Maxwell's equations using simulated and experimentally generated data, see, e.g., [1, 2, 5, 6, 7, 10, 32, 33]. In this

study we derive optimal a priori and a posteriori convergence rates for the P1 finite element scheme, for the time harmonic Maxwell system, assuming a constant dielectric permittivity function at a boundary neighborhood, hence with no in- and outflow.

An outline of this paper is as follows. In Section 2 we introduce the mathematical model and present the Cauchy problem for the time harmonic Maxwell's equations, where we assumed no dielectric volume charge. In Section 3 we describe variational method for the stabilized model, set up the finite element scheme and prove its well-posedness. Section 4 is devoted to the error analysis, where optimal a priori and a posteriori error estimates are derived in a, gradient dependent, triple norm of Sobolev type. In the a posteriori case the boundary residual, containing a normal derivative, is balanced by a multiplicative positive power of the mesh parameter. Further regularity assumptions on the solution of a dual problem yields a superconvergence for the a posteriori error estimate of order $\mathcal{O}(h^{3/2})$. An adaptivity algorithm is presented in order to reach an adequate stopping criterion in iterative mesh-generation procedure. Section 5 is devoted to implementations that justify the theoretical/approximative achievements in the paper. Finally, in Section 6 we conclude the results of the paper.

Throughout this paper C denotes a generic constant, not necessarily the same at each occurrence and independent of the mesh parameter, the solution and other involved parameters, unless otherwise specifically specified.

2 The mathematical model

The original model here is given in terms of the electric field $\hat{E}(x, s)$, $x \in \mathbb{R}^d$, $d = 2, 3$ and is varying with the pseudo-frequency $s > \text{const.} > 0$, see [5], under the assumption that the magnetic permeability of the medium is $\mu \equiv 1$. We consider the Cauchy problem for the time-harmonic Maxwell's equations for electric field $\hat{E}(x, s)$ under the assumption of the vanishing electric volume charges. Hence, the corresponding equation is then given by

$$\begin{aligned} s^2 \varepsilon(x) \hat{E}(x, s) + \nabla \times \nabla \times \hat{E}(x, s) &= s \varepsilon(x) f_0(x), \quad x \in \mathbb{R}^d, d = 2, 3 \\ \nabla \cdot (\varepsilon(x) \hat{E}(x, s)) &= 0. \end{aligned} \quad (2.1)$$

Here, $\varepsilon(x) = \varepsilon_r(x) \varepsilon_0$ is the dielectric permittivity function, $\varepsilon_r(x)$ is the dimensionless relative dielectric permittivity function and ε_0 is the permittivity of the free space, and

$$\nabla \times \nabla \times E = \nabla(\nabla \cdot E) - \nabla^2 E. \quad (2.2)$$

The model equation (2.1) can be obtained by applying the Laplace transform in time, viz.

$$\hat{E}(x, s) := \int_0^{+\infty} E(x, t) e^{-st} dt, \quad s = \text{const.} > 0 \quad (2.3)$$

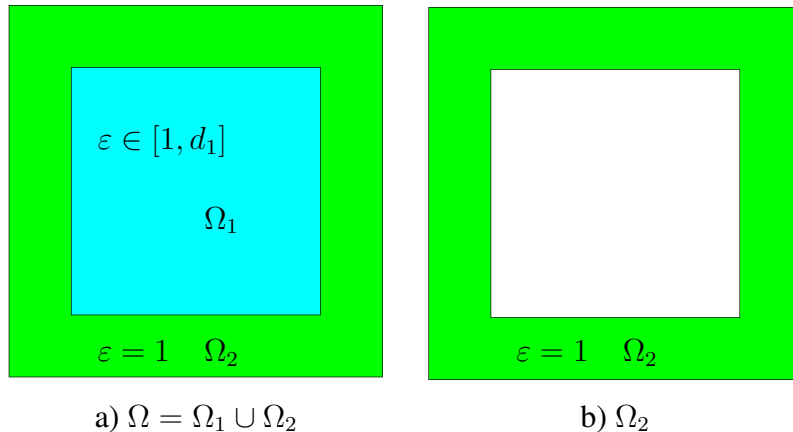


Figure 1: *Domain decomposition in Ω .*

to the function $E(x, t)$ satisfying the time-dependent Maxwell's equations

$$\begin{aligned}
 \varepsilon(x) \frac{\partial^2 E(x, t)}{\partial t^2} + \nabla \times \nabla \times E(x, t) &= 0, \quad x \in \mathbb{R}^d, d = 2, 3, t \in (0, T]. \\
 \nabla \cdot (\varepsilon E)(x, t) &= 0, \\
 E(x, 0) = f_0(x), \quad \frac{\partial E}{\partial t}(x, 0) &= 0, \quad x \in \mathbb{R}^d, \quad d = 2, 3.
 \end{aligned} \tag{2.4}$$

In the problem (2.4) we consider non-zero initial condition $E(x, 0) = f_0(x)$ which is important for solution of coefficient inverse problem for determination of the function $\varepsilon(x)$ from finite number of observations at the boundary. This condition gives stability estimate and uniqueness of the reconstruction of the function $\varepsilon(x)$ using finite number of observations of the electric field $E(x, t)$ at the small neighborhood of the boundary Γ , see details in [8].

We are not able, numerically, solve the problem (2.4) in unbounded domains and thus introduce a convex bounded, polygonal, subdomain $\Omega \subset \mathbb{R}^d, d = 2, 3$ with boundary Γ : More specifically, Ω is a simply connected domain. We define $\Omega_2 := \Omega \setminus \Omega_1$, where $\Omega_1 \subset \Omega$ has positive Lebesgue measure and $\partial\Omega \cap \partial\Omega_1 = \emptyset$. In this way cutting out Ω_1 from Ω , the new subdomain Ω_2 shares the boundary with both Ω and Ω_1 : $\partial\Omega_2 = \partial\Omega \cup \partial\Omega_1$, $\Omega = \Omega_1 \cup \Omega_2$, $\Omega_1 = \Omega \setminus \Omega_2$ and $\bar{\Omega}_1 \cap \bar{\Omega}_2 = \partial\Omega_1$, (see the Fig. 1).

To proceed we assume that $\varepsilon(x) \in C^2(\mathbb{R}^d), d = 2, 3$ and for some known constant $d_1 > 1$,

$$\begin{aligned}
 \varepsilon(x) &\in [1, d_1], & \text{for } x &\in \Omega_1, \\
 \varepsilon(x) &= 1, & \text{for } x &\in \Omega \setminus \Omega_1, \\
 \partial_\nu \varepsilon &= 0, & \text{for } x &\in \partial\Omega_2.
 \end{aligned} \tag{2.5}$$

Remark 2.1. Conditions (2.5) mean that, in the vicinity of the boundary of the computational domain Ω , the equation (2.4) transforms to the usual time-dependent wave equation.

As for $\Gamma := \partial\Omega$ the boundary of the computational domain Ω , we use the split $\Gamma = \Gamma_1 \cup \Gamma_2 \cup \Gamma_3$, so that Γ_1 and Γ_2 are the top and bottom sides, with respect to y - (in $2d$) or z -axis (in $3d$), of the domain Ω , respectively, while Γ_3 is the rest of the boundary. Further, $\partial_\nu(\cdot)$ denotes the normal derivative on Γ , where ν is the outward unit normal vector on the boundary Γ .

Remark 2.2. In most estimates below, it suffices to restrict the Neumann boundary condition for the dielectric permittivity function to: $\partial_\nu \varepsilon(x) = 0$, to $\Gamma_1 \cup \Gamma_2$. Possible usage of the general form in (2.5) will be clear from the context.

Now, using similar argument as in the studies in [1]-[7] and by Remark 2.1, for the time-dependent wave equation, we impose first order absorbing boundary condition [17] at $\Gamma_1 \cup \Gamma_2$:

$$\partial_\nu E + \partial_t E = 0, \quad (x, t) \in (\Gamma_1 \cup \Gamma_2) \times (0, T]. \quad (2.6)$$

To impose boundary conditions at Γ_3 we can assume that the surface Γ_3 is located far from the domain Ω_1 . Hence, we can assume that $E \approx E^{inc}$ in a vicinity of Γ_3 , where E^{inc} is the incident field. Thus, at Γ_3 we may impose Neumann boundary condition

$$\partial_\nu E = 0, \quad (x, t) \in \Gamma_3 \times (0, T]. \quad (2.7)$$

Finally, using the well known vector-analysis relation (2.2) and applying the Laplace transform to the equation (2.4) and the boundary conditions (2.6)-(2.7) in the time domain, the problem (2.1) will be transformed to the following model problem

$$\begin{aligned} s^2 \varepsilon(x) \hat{E}(x, s) + \nabla(\nabla \cdot \hat{E}(x, s)) - \Delta \hat{E}(x, s) &= s \varepsilon(x) f_0(x), \quad x \in \mathbb{R}^d, d = 2, 3 \\ \nabla \cdot (\varepsilon(x) \hat{E}(x, s)) &= 0, \\ \partial_\nu \hat{E}(x, s) &= 0, \quad x \in \Gamma_3, \\ \partial_\nu \hat{E}(x, s) &= f_0(x) - s \hat{E}(x, s), \quad x \in \Gamma_1 \cup \Gamma_2. \end{aligned} \quad (2.8)$$

3 Variational approach

We denote the standard inner product in $[L_2(\Omega)]^d$ as (\cdot, \cdot) , $d \in \{2, 3\}$, and the corresponding norm by $\|\cdot\|$. Similarly we denote by $\langle \cdot, \cdot \rangle_\Gamma$ the standard inner product of $[L_2(\Gamma)]^{d-1}$ and the associated $L_2(\Gamma)$ -norm by $\|\cdot\|_\Gamma$. We define the L_2 -weighted scalar product by

$$(u, v) := \int_\Omega u \cdot v \, d\mathbf{x}, \quad (u, v)_\omega := \int_\Omega u \cdot v \, \omega \, d\mathbf{x}, \quad \langle u, v \rangle_\Gamma := \int_\Gamma u \cdot v \, d\sigma,$$

and the ω -weighted $L^2(\Omega)$ norm as

$$\|u\|_\omega := \sqrt{\int_\Omega |u|^2 \, \omega \, d\mathbf{x}}, \quad \omega > 0, \quad \omega \in L^\infty(\Omega).$$

3.1 Stabilized model

The stabilized formulation of the problem (2.8), with $d = 2, 3$, is now written as:

$$\begin{aligned} s^2\varepsilon(x)\hat{E}(x, s) - \Delta\hat{E}(x, s) - \nabla(\nabla \cdot ((\varepsilon - 1)\hat{E}(x, s))) &= s\varepsilon(x)f_0(x) \quad x \in \mathbb{R}^d, \\ \partial_\nu\hat{E}(x, s) &= 0, \quad x \in \Gamma_3, \\ \partial_\nu\hat{E}(x, s) &= f_0(x) - s\hat{E}(x, s), \quad x \in \Gamma_1 \cup \Gamma_2, \end{aligned} \quad (3.1)$$

where the second equation in (2.8) is hidden in the first one above. Let us first show that the stabilized problem (3.1) is equivalent to the original one (2.8). To do this we consider the variational formulation of (3.1) for all $\mathbf{v} \in [H^1(\Omega)]^3$,

$$\begin{aligned} (s^2\varepsilon\hat{E}, \mathbf{v}) + (\nabla\hat{E}, \nabla\mathbf{v}) + (\nabla \cdot (\varepsilon\hat{E}), \nabla \cdot \mathbf{v}) - (\nabla \cdot \hat{E}, \nabla \cdot \mathbf{v}) \\ - \langle f_0, \mathbf{v} \rangle_{\Gamma_1 \cup \Gamma_2} + \langle s\hat{E}, \mathbf{v} \rangle_{\Gamma_1 \cup \Gamma_2} - \langle \nabla \cdot (\varepsilon\hat{E}) - \nabla \cdot \hat{E}, \mathbf{v} \cdot \nu \rangle_\Gamma = (s\varepsilon f_0, \mathbf{v}). \end{aligned} \quad (3.2)$$

Assumption 1. By condition (2.5) we may assume that the dielectric permittivity function $\varepsilon(x) \equiv 1$ on a neighborhood of Γ and hence the last boundary integral above is indeed $\equiv 0$. We have kept this term in order to follow the computational steps. A full consideration with varying $\varepsilon(x)$ is of vital importance for the time dependent problem and will be included in the subject of a forthcoming study. For a communication on this see, e.g., [4].

Integration by parts, in the spatial domain, in the second, third and fourth terms in the equation (3.2) yields, for all $\mathbf{v} \in [H^1(\Omega)]^3$, that

$$\begin{aligned} (s^2\varepsilon\hat{E}, \mathbf{v}) + (\nabla(\nabla \cdot \hat{E}), \mathbf{v}) - (\Delta\hat{E}, \mathbf{v}) - (\nabla(\nabla \cdot (\varepsilon\hat{E})), \mathbf{v}) - \langle f_0, \mathbf{v} \rangle_{\Gamma_1 \cup \Gamma_2} + \langle s\hat{E}, \mathbf{v} \rangle_{\Gamma_1 \cup \Gamma_2} \\ - \langle \nabla \cdot (\varepsilon\hat{E}) - \nabla \cdot \hat{E}, \mathbf{v} \cdot \nu \rangle_\Gamma + \langle \partial_\nu\hat{E}, \mathbf{v} \rangle_\Gamma + \langle \nabla \cdot (\varepsilon\hat{E}) - \nabla \cdot \hat{E}, \mathbf{v} \cdot \nu \rangle_\Gamma = (s\varepsilon f_0, \mathbf{v}), \end{aligned} \quad (3.3)$$

which can be simplified as

$$\begin{aligned} (s^2\varepsilon\hat{E}, \mathbf{v}) + (\nabla(\nabla \cdot \hat{E}), \mathbf{v}) - (\Delta\hat{E}, \mathbf{v}) - (\nabla(\nabla \cdot (\varepsilon\hat{E})), \mathbf{v}) \\ - \langle f_0, \mathbf{v} \rangle_{\Gamma_1 \cup \Gamma_2} + \langle s\hat{E}, \mathbf{v} \rangle_{\Gamma_1 \cup \Gamma_2} + \langle \partial_\nu\hat{E}, \mathbf{v} \rangle_{\Gamma_1 \cup \Gamma_2} = (s\varepsilon f_0, \mathbf{v}), \quad \forall \mathbf{v} \in [H^1(\Omega)]^3. \end{aligned} \quad (3.4)$$

Using the conditions (2.5) we get from the above equation that

$$\begin{aligned} s^2\varepsilon\hat{E} + \nabla(\nabla \cdot \hat{E}) - \Delta\hat{E} - \nabla(\nabla \cdot (\varepsilon\hat{E})) &= s\varepsilon f_0 \quad \text{in } \Omega, \\ \partial_\nu\hat{E} &= f_0 - s\hat{E} \quad \text{on } \Gamma_1 \cup \Gamma_2, \\ \partial_\nu\hat{E} &= 0 \quad \text{on } \Gamma_3. \end{aligned} \quad (3.5)$$

From this equation it follows that $\nabla \cdot (\varepsilon\hat{E}) = 0$. To see it, we let \tilde{E} be the unique solution of the problem (2.8) and consider the difference $\bar{E} = \hat{E} - \tilde{E}$ between the solution \hat{E} of the

problem (3.5) and the solution \tilde{E} of the problem (2.8). We observe that the function \bar{E} is the solution of the following boundary value problem:

$$\begin{aligned} s^2 \varepsilon \bar{E} - \Delta \bar{E} - \nabla(\nabla \cdot ((\varepsilon - 1)\bar{E})) &= 0 && \text{in } \Omega, \\ \partial_\nu \bar{E} &= -s\bar{E} && \text{on } \Gamma_1 \cup \Gamma_2, \\ \partial_\nu \bar{E} &= 0 && \text{on } \Gamma_3. \end{aligned} \quad (3.6)$$

Now we multiply the equation (3.6) by $\mathbf{v} \in [H^1(\Omega)]^3$ and integrate over Ω to get:

$$(s^2 \varepsilon \bar{E}, \mathbf{v}) + (\nabla \bar{E}, \nabla \mathbf{v}) + ((\varepsilon - 1)\nabla \cdot \bar{E}, \nabla \cdot \mathbf{v}) + \langle s\bar{E}, \mathbf{v} \rangle_{\Gamma_1 \cup \Gamma_2} = 0 \quad \text{in } \Omega. \quad (3.7)$$

Using $\mathbf{v} = \bar{E}$ (3.7), performing the integration over Ω and taking into account the condition that $\varepsilon(x) \equiv 0$ in the vicinity of Γ hence, $(\nabla \cdot ((\varepsilon - 1)\bar{E}), \nabla \cdot \bar{E})_\Omega = 0$, we get

$$(s^2 \varepsilon \bar{E}, \bar{E}) + (\nabla \bar{E}, \nabla \bar{E}) + ((\varepsilon - 1)\nabla \cdot \bar{E}, \nabla \cdot \bar{E}) + \langle s\bar{E}, \bar{E} \rangle_{\Gamma_1 \cup \Gamma_2} = 0 \quad \text{in } \Omega, \quad (3.8)$$

or, equivalently,

$$\| \bar{E} \|_{s^2 \varepsilon}^2 + \| \nabla \bar{E} \|^2 + \| \nabla \cdot \bar{E} \|_{(\varepsilon - 1)}^2 + \| \bar{E} \|_{s, \Gamma_1 \cup \Gamma_2}^2 = 0. \quad (3.9)$$

From (3.9) we see that $\bar{E} \equiv 0$ and hence, $\hat{E} = \tilde{E}$, or the solution \hat{E} of the stabilized problem (3.5) is the same as the solution \tilde{E} of the original problem (2.8).

3.2 Finite element discretization

We consider a partition of Ω into elements K denoted by $\mathcal{T}_h = \{K\}$, satisfying the standard finite element subdivision with the minimal angle condition of elements $K \in \mathcal{T}_h$. Here, $h = h(x)$ is a mesh function defined as $h|_K = h_K$, representing the local diameter of the elements. We also denote by $\partial\mathcal{T}_h = \{\partial K\}$ a partition of the boundary Γ into boundaries ∂K of the elements K such that vertices of these elements belong to Γ . Note that, although Γ is polygonal (in $2d$) or plans-surface ($3d$) domain, it is a priori the case that $\partial K \subset \Gamma$, hence to fix this, some further subdivision might be necessary.

To formulate the finite element method for (3.1) in Ω , we introduce the, piecewise linear, finite element space $W_h^E(\Omega)$ for every component of the electric field E defined by

$$W_h^E(\Omega) := \{w \in H^1(\Omega) : w|_K \in P_1(K), \forall K \in \mathcal{T}_h\},$$

where $P_1(K)$ denote the set of piecewise-linear functions on K . Setting $\mathbf{W}_h^E(\Omega) := [W_h^E(\Omega)]^3$ we define f_{0h} to be the usual \mathbf{W}_h^E -interpolant of f_0 in (3.1). Then the finite element method for the problem (3.1) in Ω is formulated as:

Find $\hat{E}_h \in \mathbf{W}_h^E(\Omega)$ such that $\forall \mathbf{v} \in \mathbf{W}_h^E(\Omega)$

$$\begin{aligned} (s^2 \varepsilon \hat{E}_h, \mathbf{v}) + (\nabla \hat{E}_h, \nabla \mathbf{v}) + (\nabla \cdot (\varepsilon \hat{E}_h), \nabla \cdot \mathbf{v}) - (\nabla \cdot \hat{E}_h, \nabla \cdot \mathbf{v}) \\ + \langle s\hat{E}_h, \mathbf{v} \rangle_{\Gamma_1 \cup \Gamma_2} = (s\varepsilon f_{0h}, \mathbf{v}) + \langle f_{0h}, \mathbf{v} \rangle_{\Gamma_1 \cup \Gamma_2}. \end{aligned} \quad (3.10)$$

Remark 3.1. Recalling the Assumption 1, the boundary term: $\langle \nabla \cdot (\varepsilon \hat{E}) - \nabla \cdot \hat{E} \rangle_\Gamma$ present in (3.2) and (3.3) vanishes and hence does not appear in (3.10) and the subsequent relations.

Theorem 1 (well-posedness). *The problem (3.10) has a unique solution $\hat{E}_h \in \mathbf{W}_h^E(\Omega)$.*

Proof. We define the bilinear and linear forms, respectively, as

$$\begin{aligned} a(\hat{E}_h, \mathbf{v}) = & (s^2 \varepsilon \hat{E}_h, \mathbf{v}) + (\nabla \hat{E}_h, \nabla \mathbf{v}) + (\nabla \cdot (\varepsilon \hat{E}_h), \nabla \cdot \mathbf{v}) \\ & - (\nabla \cdot \hat{E}_h, \nabla \cdot \mathbf{v}) + \langle s \hat{E}_h, \mathbf{v} \rangle_{\Gamma_1 \cup \Gamma_2} \end{aligned} \quad (3.11)$$

and

$$\mathcal{L}(\mathbf{v}) := (s \varepsilon f_{0,h}, \mathbf{v}) + \langle f_{0,h}, \mathbf{v} \rangle_{\Gamma_1 \cup \Gamma_2},$$

and restate the equation (3.10) in its compact form as

$$a(\hat{E}_h, \mathbf{v}) = \mathcal{L}(\mathbf{v}). \quad (3.12)$$

Now the well-posedness rely on the Lax-Milgram approach based on showing that $a(\cdot, \cdot)$ is coercive and both $a(\cdot, \cdot)$ and $\mathcal{L}(\cdot)$ are continuous. To this end we introduce the triple norm

$$|||\hat{E}_h|||^2 := \|\hat{E}_h\|_{s^2 \varepsilon}^2 + \|\nabla \hat{E}_h\|^2 + \|\nabla \cdot \hat{E}_h\|_{\varepsilon^{-1}}^2 + \|\hat{E}_h\|_{s, \Gamma_1 \cup \Gamma_2}^2$$

and show that there are constants C_i , $i = 1, 2, 3$ such that for all \hat{E}_h and $\mathbf{v} \in \mathbf{W}_h^E(\Omega)$,

$$a(\hat{E}_h, \hat{E}_h) \geq C_1 |||\hat{E}_h|||^2, \quad (\text{Coercivity}), \quad (3.13)$$

$$a(\hat{E}_h, \mathbf{v}) \leq C_2 |||\hat{E}_h||| \cdot |||\mathbf{v}|||, \quad (\text{Continuity of } a), \quad (3.14)$$

$$|\mathcal{L}(\mathbf{v})| \leq C_3 |||\mathbf{v}|||, \quad (\text{Continuity of } \mathcal{L}) \quad (3.15)$$

The first relation is straightforward and in fact an equality holds with $C_1 = 1$, viz.

$$a(\hat{E}_h, \hat{E}_h) \equiv |||\hat{E}_h|||^2.$$

The continuity of $a(\cdot, \cdot)$ is evident from the fact that, for every $\mathbf{v} \in \mathbf{W}_h^E(\Omega)$, using *Cauchy-Schwarz' inequality*, we have that

$$\begin{aligned} a(\hat{E}_h, \mathbf{v}) = & (s\sqrt{\varepsilon} \hat{E}_h, s\sqrt{\varepsilon} \mathbf{v}) + (\nabla \hat{E}_h, \nabla \mathbf{v}) \\ & + (\nabla \cdot (\sqrt{\varepsilon - 1} \hat{E}_h), \nabla \cdot (\sqrt{\varepsilon - 1} \mathbf{v})) + \langle \sqrt{s} \hat{E}_h, \sqrt{s} \mathbf{v} \rangle_{\Gamma_1 \cup \Gamma_2} \\ \leq & \|\hat{E}_h\|_{s^2 \varepsilon} \|\mathbf{v}\|_{s^2 \varepsilon} + \|\nabla \hat{E}_h\| \|\nabla \mathbf{v}\| + \|\nabla \cdot \hat{E}_h\|_{\varepsilon^{-1}} \|\nabla \cdot \mathbf{v}\|_{\varepsilon^{-1}} \\ & + \|\hat{E}_h\|_{s, \Gamma_1 \cup \Gamma_2} \|\mathbf{v}\|_{s, \Gamma_1 \cup \Gamma_2} \leq |||\hat{E}_h||| \cdot |||\mathbf{v}|||. \end{aligned} \quad (3.16)$$

Likewise, for $f_{0,h} \in L_{2,\varepsilon}(\Omega) \cap L_{2,1/s}(\Gamma_1 \cup \Gamma_2)$ we can easily verify that

$$\begin{aligned} \mathcal{L}(\mathbf{v}) = & \left(\sqrt{\varepsilon} f_{0,h}, s\sqrt{\varepsilon} \mathbf{v} \right) + \langle f_{0,h}, \mathbf{v} \rangle_{\Gamma_1 \cup \Gamma_2} \\ \leq & \|f_{0,h}\|_\varepsilon \|\mathbf{v}\|_{s^2 \varepsilon} + \|f_{0,h}\|_{1/s, \Gamma_1 \cup \Gamma_2} \|\mathbf{v}\|_{s, \Gamma_1 \cup \Gamma_2} \\ \leq & \left(\|f_{0,h}\|_\varepsilon + \|f_{0,h}\|_{1/s, \Gamma_1 \cup \Gamma_2} \right) |||\mathbf{v}|||, \end{aligned} \quad (3.17)$$

and hence \mathcal{L} is continuous as well. Summing up, by the coercivity (3.13) and the continuities (3.16) and (3.17) we may use the Lax-Milgram theorem which guarantee's the existence of a unique solution for the discrete problem (3.10). The continuities would yield even stability and hence justifies the well-posedness and completes the proof. \square

4 Error analysis

In this section first we give a swift a priori error bound and then continue with a posteriori error estimates and derive a corresponding adaptive algorithm for the above, piecewise linear approximation of the time harmonic Maxwell's equations formulated in (3.10).

4.1 A priori error estimates

To derive a priori error estimates we need to define a continuous version of the linear and bilinear forms introduced in well-posedness theorem. To this end, we rewrite (3.11) replacing \hat{E}_h by \hat{E} and with a new continuous linear form defined with same expression as $\mathcal{L}(\mathbf{v})$, but for $\mathbf{v} \in H^1(\Omega)$ rather than in the finite element space $\mathbf{W}_h^E(\Omega)$:

$$\begin{aligned} a(\hat{E}, \mathbf{v}) = & (s^2 \varepsilon \hat{E}, \mathbf{v}) + (\nabla \hat{E}, \nabla \mathbf{v}) + (\nabla \cdot (\varepsilon \hat{E}), \nabla \cdot \mathbf{v}) \\ & - (\nabla \cdot \hat{E}, \nabla \cdot \mathbf{v}) + \langle s \hat{E}, \mathbf{v} \rangle_{\Gamma_1 \cup \Gamma_2}, \quad \forall \mathbf{v} \in H^1(\Omega) \end{aligned} \quad (4.1)$$

and

$$\mathcal{L}^c(\mathbf{v}) := (s \varepsilon f_0, \mathbf{v}) + \langle f_0, \mathbf{v} \rangle_{\Gamma_1 \cup \Gamma_2}, \quad \forall \mathbf{v} \in H^1(\Omega). \quad (4.2)$$

Hence we have the concise form of the variational formulation

$$a(\hat{E}, \mathbf{v}) = \mathcal{L}^c(\mathbf{v}), \quad \forall \mathbf{v} \in H^1(\Omega). \quad (4.3)$$

To proceed we derive *Galerkin orthogonality* relation by letting, in (4.1) and (4.2), $\mathbf{v} \in \mathbf{W}_h^E(\Omega)$, as well as replacing f_0 by $f_{0,h}$ in (4.2). Subtracting (3.12) from the, such obtained, continuous problem (4.3) and letting $e(x, s) := \hat{E}(x, s) - \hat{E}_h(x, s)$ be the pointwise spatial error of the finite element approximation (3.10), we get

$$a(\hat{E} - \hat{E}_h, \mathbf{v}) = 0, \quad \forall \mathbf{v} \in \mathbf{W}_h^E(\Omega), \quad (\text{Galerkin orthogonality}). \quad (4.4)$$

Note that restricting (4.3) to $\mathbf{v} \in \mathbf{W}_h^E(\Omega)$, (3.12) and (4.3) get the same right hand sides.

Now we are ready to derive the following theoretical error bound

Theorem 2. *Let \hat{E} and \hat{E}_h be the solutions for the continuous problem (3.1) (in the variational form (3.2)) and its finite element approximation, (3.10), respectively. Then, there is a constant C , independent of \hat{E} and h , such that*

$$\|e\| \leq C \|h \hat{E}\|_{H_w^2(\Omega)}.$$

where $w = w(\varepsilon(x), s)$ is the weight function which depends on the dielectric permittivity function $\varepsilon(x)$ and the pseudo-frequency variable s .

Proof. Using the definition of the triple norm and Galerkin orthogonality (4.4) we have

$$\|e\|^2 = a(e, e) = a(e, \hat{E} - \hat{E}_h) = a(e, \hat{E}) = a(e, \hat{E} - \mathbf{v}), \quad \forall \mathbf{v} \in \mathbf{W}_h^E(\Omega). \quad (4.5)$$

Now we set $\mathbf{v} := \pi_h \hat{E}$, the interpolant of \hat{E} . Then, using the Cauchy-Schwarz' inequality and the interpolation error estimates we can estimate the right hand side of (4.5) as follows:

$$\begin{aligned} \|e\|^2 &= (e, \hat{E} - \pi_h \hat{E})_{s^2\varepsilon} + (\nabla e, \nabla(\hat{E} - \pi_h \hat{E})) \\ &\quad + (\nabla \cdot e, \nabla \cdot (\hat{E} - \pi_h \hat{E}))_{\varepsilon-1} + \langle e, \hat{E} - \pi_h \hat{E} \rangle_{s, \Gamma_1 \cup \Gamma_2} \\ &\leq \|e\|_{s^2\varepsilon} \|\hat{E} - \pi_h \hat{E}\|_{s^2\varepsilon} + \|\nabla e\| \|\nabla(\hat{E} - \pi_h \hat{E})\| \\ &\quad + \|\nabla \cdot e\|_{\varepsilon-1} \|\nabla \cdot (\hat{E} - \pi_h \hat{E})\|_{\varepsilon-1} + \|e\|_{s, \Gamma_1 \cup \Gamma_2} \|\hat{E} - \pi_h \hat{E}\|_{s, \Gamma_1 \cup \Gamma_2} \\ &\leq C_1 \|e\|_{s^2\varepsilon} \|h^2 D^2 \hat{E}\|_{s^2\varepsilon} + C_2 \|\nabla e\| \|h D^2 \hat{E}\| + \\ &\quad + C_2 \|\nabla \cdot e\|_{\varepsilon-1} \|h D^2 \hat{E}\|_{\varepsilon-1} + \\ &\quad + C_3 \|e\|_{s, \Gamma_1 \cup \Gamma_2} \left(\|h^2 D^2 \hat{E}\|_{s, L_2(\Omega)}^{1/2} \cdot \|h D^2 \hat{E}\|_{s, L_2(\Omega)}^{1/2} \right) \\ &\leq C \|e\| \cdot \left(\|h^2 D^2 \hat{E}\|_{s^2\varepsilon} + \|h D^2 \hat{E}\| + \|h D^2 \hat{E}\|_{\varepsilon-1} + \right. \\ &\quad \left. + \|h^{3/2} D^2 \hat{E}\|_s \right) \leq C \|e\| \cdot \|h D^2 \hat{E}\|_w, \end{aligned} \quad (4.6)$$

where $w = \max(hs^2\varepsilon, h^{1/2}(\varepsilon - 1), h^{1/2}s)$, and to estimate the interpolation error at the boundary we apply the Poincare inequality (since $\hat{E} - \pi_h \hat{E} = 0$ on the whole or part of Γ with positive Lebesgue measure) to the trace estimate (see Brenner-Scott [9]; Theorem 1.6.6):

$$\begin{aligned} \|\hat{E} - \pi_h \hat{E}\|_{s, \Gamma} &\leq \tilde{C} \|\hat{E} - \pi_h \hat{E}\|_{s, L_2(\Omega)}^{1/2} \|\hat{E} - \pi_h \hat{E}\|_{s, H^1(\Omega)}^{1/2} \\ &\leq \tilde{C} \|\hat{E} - \pi_h \hat{E}\|_{s, L_2(\Omega)}^{1/2} \|\nabla(\hat{E} - \pi_h \hat{E})\|_{s, L_2(\Omega)}^{1/2} \\ &\leq \tilde{C} \|h^2 D^2 \hat{E}\|_{s, L_2(\Omega)}^{1/2} \cdot \|h D^2 \hat{E}\|_{s, L_2(\Omega)}^{1/2} \end{aligned} \quad (4.7)$$

where D^2 stands for the differential operator which, e.g., for the 2-dimensional domain Ω , i.e., in xy -geometry and for $u \in C^{(2)}(\Omega)$ is given by

$$D^2 u := (u_{xx}^2 + 2u_{xy}^2 + u_{yy}^2)^{1/2}.$$

Finally $C = \max C_i$, $i = 1, 2$ are the interpolation constants and $C_3 = \tilde{C}(C_1 + C_2)$ and the proof is complete. \square

Remark 4.1. We note that the obtained error is of order $\mathcal{O}(h)$ in $H_w^2(\Omega)$ which is optimal due to the gradient term in the triple norm. This may be further improved, to achieve superconvergence and estimations in the negative norm which in scalar form is defined as

$$\|w\|_{H^{-s}(\Omega)} = \sup_{\varphi \in H^s(\Omega) \cap H_0^1(\Omega)} \frac{(w, \varphi)}{\|\varphi\|_{H^s(\Omega)}}.$$

This, however, extended to vector form, yields extra computational complexity. Otherwise, *with no gradient term*, using the Laplace transform, the equation is rendered from being hyperbolic to an elliptic one and the trace theorem estimating the boundary integrals is the term setting an upper limit of $\mathcal{O}(h^{3/2})$. This however, would not survive due to the fact that the triple norm involves gradient norm and the optimal order is indeed $\mathcal{O}(h)$, (rather than $\mathcal{O}(h^2)$ of the purely L_2 -norm).

4.2 A posteriori error estimates

For the approximate solution $\hat{E}_h = \hat{E}_h(x, s)$ of the problem (3.1), where $x \in \Omega \subset \mathbb{R}^d$, $d = 2, 3$, we define the residual errors, viz.

$$\begin{aligned} -\mathcal{R}(\hat{E}_h) &:= s^2 \varepsilon(x) \hat{E}_h - \Delta \hat{E}_h - \nabla(\nabla \cdot ((\varepsilon(x) - 1) \hat{E}_h) - s \varepsilon(x) f_{0,h}(x)), \quad \text{and} \\ -\mathcal{R}_\Gamma(\hat{E}_h) &:= h^{-\alpha} \left(\partial_\nu \hat{E}_h + s \hat{E}_h - f_{0,h}(x) \right), \quad \text{for } x \in \Gamma_1 \cup \Gamma_2, \quad 0 < \alpha \leq 1. \end{aligned} \quad (4.8)$$

By the Galerkin orthogonality we have that $\mathcal{R}(\hat{E}_h) \perp \mathbf{W}_h^E(\Omega)$. Now the objective is to bound the triple norm of the error $e(x, s) := \hat{E}(x, s) - \hat{E}_h(x, s)$ by some adequate norms of $\mathcal{R}(\hat{E}_h)$ and $\mathcal{R}_\Gamma(\hat{E}_h)$ with a relevant, fast, decay. This may be done in a few, relatively similar, ways, e.g., one can use the variational formulation and interpolation in the error combined with Galerkin orthogonality. Or one may use a dual problem approach setting the source term (or initial data) as the error. We check both techniques to the time harmonic Maxwell's equations. The former is given in the Theorem 3 below and the latter is the subject of Proposition 4.2. The proof of the main theorem will rely on assuming a first order approximation for the initial value of the original field $f_0(x) := E(x, t)|_{t=0_-}$, for $\beta \approx 1$, and according to

$$\|f_0 - f_{0,h}\|_\varepsilon \approx \|f_0 - f_{0,h}\|_{1/s, \Gamma} \approx \|f_0 - f_{0,h}\|_{(\varepsilon-1)^2/s, \Gamma} = \mathcal{O}(h^\beta). \quad (4.9)$$

The justification for (4.9) is that f_0 , as the time independent field $E(x, 0)$ satisfies a Poisson type equation and, tackling the contributions from the weights, a finite element bound of the form (4.9) is evident.

Theorem 3. Let \hat{E} and \hat{E}_h be the solutions for the continuous problem (3.1) (in the variational form (3.2)) and its finite element approximation (3.10), respectively. Further we

assume that we have the error bound (4.9) for the initial field $f_0(x) := E(x, t)|_{t=0_-}$. Then, there exist interpolation constants C_1 and C_2 , independent of h , and \hat{E} , but may depend on ε and s such that the following a posteriori error estimate holds true

$$|||e||| \leq C_1 h \|\mathcal{R}\| + C_2 h^\alpha \|\mathcal{R}_\Gamma\|_{1/s, \Gamma_1 \cup \Gamma_2} + \mathcal{O}(h^\beta), \quad (4.10)$$

where $\alpha \approx \beta \approx 1$.

Proof. We shall use the weak form emerging from the triple norm of the error where the contribution from the ∂_ν will be canceled using Green's formula to the Laplacian

$$\begin{aligned} |||e|||^2 &= (s^2 \varepsilon e, e) + (\nabla e, \nabla e) + (\nabla \cdot ((\varepsilon - 1)e), \nabla \cdot e) + \langle s e, e \rangle_{\Gamma_1 \cup \Gamma_2} \\ &\quad - \langle \nabla \cdot (\varepsilon e), e \rangle_\Gamma + \langle \nabla \cdot (\varepsilon e), e \rangle_\Gamma := \sum_{j=1}^4 I_j. \end{aligned} \quad (4.11)$$

Now by the Green's formula and the fact that $\partial_\nu e \equiv 0$ on Γ_3 , we have

$$\begin{aligned} I_2 + I_3 &= -(\Delta e, e) - (\nabla(\nabla \cdot ((\varepsilon - 1)e)), e) \\ &\quad + \langle \partial_\nu e, e \rangle_{\Gamma_1 \cup \Gamma_2} + \langle \partial_\nu((\varepsilon - 1)e), e \rangle_{\Gamma_1 \cup \Gamma_2} \\ &= -(\Delta e, e) - \nabla(\nabla \cdot ((\varepsilon - 1)e), e) + \langle \partial_\nu(\varepsilon e), e \rangle_{\Gamma_1 \cup \Gamma_2}. \end{aligned} \quad (4.12)$$

Hence

$$\begin{aligned} |||e|||^2 &= (s^2 \varepsilon e, e) - (\Delta e, e) - \nabla(\nabla \cdot ((\varepsilon - 1)e), e) \\ &\quad + \langle \partial_\nu(\varepsilon e), e \rangle_{\Gamma_1 \cup \Gamma_2} + \langle s e, e \rangle_{\Gamma_1 \cup \Gamma_2} \end{aligned} \quad (4.13)$$

Thus, recalling the definition of the residuals \mathcal{R} and \mathcal{R}_Γ , we can write

$$\begin{aligned} |||e|||^2 &= (s^2 \varepsilon \hat{E} - \Delta \hat{E} - \nabla(\nabla \cdot ((\varepsilon - 1)\hat{E})), e) + \langle \partial_\nu(\varepsilon \hat{E}), e \rangle_{\Gamma_1 \cup \Gamma_2} + \langle s \hat{E}, e \rangle_{\Gamma_1 \cup \Gamma_2} \\ &\quad - (s^2 \varepsilon \hat{E}_h - \Delta_h \hat{E}_h - \nabla_h(\nabla \cdot ((\varepsilon - 1)\hat{E}_h)), e) - \langle \partial_\nu(\varepsilon \hat{E}_h), e \rangle_{\Gamma_1 \cup \Gamma_2} - \langle s \hat{E}_h, e \rangle_{\Gamma_1 \cup \Gamma_2} \\ &= (s \varepsilon f_0, e) + (\mathcal{R}(\hat{E}_h), e) - (s \varepsilon f_{0,h}, e) + \langle \partial_\nu((\varepsilon - 1)\hat{E}), e \rangle_{\Gamma_1 \cup \Gamma_2} + \langle \partial_\nu \hat{E}, e \rangle_{\Gamma_1 \cup \Gamma_2} \\ &\quad + \langle s \hat{E}, e \rangle_{\Gamma_1 \cup \Gamma_2} - \langle \partial_\nu((\varepsilon - 1)\hat{E}_h), e \rangle_{\Gamma_1 \cup \Gamma_2} - \langle \partial_\nu \hat{E}_h, e \rangle_{\Gamma_1 \cup \Gamma_2} - \langle s \hat{E}_h, e \rangle_{\Gamma_1 \cup \Gamma_2} \\ &= (s \varepsilon (f_0 - f_{0,h}), e) + (\mathcal{R}(\hat{E}_h), e) + \langle \partial_\nu((\varepsilon - 1)(\hat{E} - \hat{E}_h)), e \rangle_{\Gamma_1 \cup \Gamma_2} \\ &\quad + \langle h^\alpha \mathcal{R}_\Gamma(\hat{E}_h), e \rangle_{\Gamma_1 \cup \Gamma_2} + \langle f_0 - f_{0,h}, e \rangle_{\Gamma_1 \cup \Gamma_2}, \end{aligned} \quad (4.14)$$

where the contributions from the Γ_3 to the boundary terms are all identically zero. Further, we use the orthogonality relation $\mathcal{R}(\hat{E}_h) \perp \mathbf{W}_h^E(\Omega)$, so that

$$\begin{aligned} |||e|||^2 &= (\sqrt{\varepsilon}(f_0 - f_{0,h}), s\sqrt{\varepsilon}e) + (\mathcal{R}(\hat{E}_h), e - \pi_h e) \\ &\quad + \langle \partial_\nu((\varepsilon - 1)(\hat{E} - \hat{E}_h)), e \rangle_{\Gamma_1 \cup \Gamma_2} + \langle h^\alpha \mathcal{R}_\Gamma(\hat{E}_h), e \rangle_{\Gamma_1 \cup \Gamma_2} \\ &\quad + \left\langle \frac{1}{\sqrt{s}}(f_0 - f_{0,h}), \sqrt{s}e \right\rangle_{\Gamma_1 \cup \Gamma_2} := \sum_{j=1}^5 J_j \end{aligned} \quad (4.15)$$

Now we estimate each J_j -term separately

$$J_1 := (\sqrt{\varepsilon}(f_0 - f_{0,h}), s\sqrt{\varepsilon}e) \leq \|f_0 - f_{0,h}\|_\varepsilon \cdot \|e\|_{\varepsilon s^2}$$

Using the interpolation estimates

$$\begin{aligned} J_2 + J_4 &:= (\mathcal{R}(\hat{E}_h), e - \pi_h e) + \langle h^\alpha \mathcal{R}_\Gamma(\hat{E}_h), e \rangle_{\Gamma_1 \cup \Gamma_2} \\ &\leq \left(\|h\mathcal{R}(\hat{E}_h)\| \|\nabla e\| + \|h^\alpha \mathcal{R}_\Gamma(\hat{E}_h)\|_{1/s, \Gamma_1 \cup \Gamma_2} \|e\|_{s, \Gamma_1 \cup \Gamma_2} \right). \end{aligned} \quad (4.16)$$

Finally

$$J_5 := \left\langle \frac{1}{\sqrt{s}}(f_0 - f_{0,h}) + \sqrt{s}e \right\rangle_\Gamma \leq \|f_0 - f_{0,h}\|_{1/s, \Gamma_1 \cup \Gamma_2} \|e\|_{s, \Gamma_1 \cup \Gamma_2}. \quad (4.17)$$

It remains to bound the term J_3 , to this end we use the fact that $\partial_\nu \varepsilon = 0$ and hence

$$\begin{aligned} J_3 &= \langle \partial_\nu((\varepsilon - 1)(\hat{E} - \hat{E}_h)), e \rangle_\Gamma = \langle (\partial_\nu \varepsilon)(\hat{E} - \hat{E}_h), e \rangle_\Gamma + \langle (\varepsilon - 1)\partial_\nu(\hat{E} - \hat{E}_h), e \rangle_\Gamma \\ &= \langle (\varepsilon - 1)\partial_\nu(\hat{E} - \hat{E}_h), e \rangle_\Gamma. \end{aligned}$$

Using both continuous and discrete boundary conditions we have

$$\partial_\nu(\hat{E} - \hat{E}_h) = (f_0 - f_{0,h}) - s(\hat{E} - \hat{E}_h) \quad \text{on } \Gamma_1 \cup \Gamma_2,$$

and

$$\partial_\nu(\hat{E} - \hat{E}_h) = 0 \quad \text{on } \Gamma_3,$$

we can estimate J_3 as follows

$$\begin{aligned} J_3 &= \langle (\varepsilon - 1)\partial_\nu(\hat{E} - \hat{E}_h), e \rangle_{\Gamma_1 \cup \Gamma_2} \\ &= \langle (\varepsilon - 1)(f_0 - f_{0,h}) \frac{1}{\sqrt{s}}, \sqrt{s}e \rangle_{\Gamma_1 \cup \Gamma_2} - \langle (\varepsilon - 1)se, e \rangle_{\Gamma_1 \cup \Gamma_2} \\ &\leq \|f_0 - f_{0,h}\|_{(\varepsilon-1)^2/s, \Gamma_1 \cup \Gamma_2} \|e\|_{s, \Gamma_1 \cup \Gamma_2} - \min |\varepsilon - 1| \|e\|_{s, \Gamma_1 \cup \Gamma_2}. \end{aligned} \quad (4.18)$$

Summing up we have

$$\begin{aligned} |||e|||^2 &\leq \|h\mathcal{R}(\hat{E}_h)\| \|\nabla e\| + \|h^\alpha \mathcal{R}_\Gamma(\hat{E}_h)\|_{1/s, \Gamma_1 \cup \Gamma_2} \|e\|_{s, \Gamma_1 \cup \Gamma_2} \\ &\quad + \|f_0 - f_{0,h}\|_\varepsilon \|e\|_{\varepsilon s^2} + \|f_0 - f_{0,h}\|_{1/s, \Gamma_1 \cup \Gamma_2} \|e\|_{s, \Gamma_1 \cup \Gamma_2} \\ &\quad + \|f_0 - f_{0,h}\|_{(\varepsilon-1)^2/s, \Gamma_1 \cup \Gamma_2} \|e\|_{s, \Gamma_1 \cup \Gamma_2} - \min |\varepsilon - 1| \|e\|_{s, \Gamma_1 \cup \Gamma_2}. \end{aligned} \quad (4.19)$$

Now recalling (4.9), by a ‘‘kick-back’’ of the negative term $-\min |\varepsilon - 1| \|e\|_{s, \Gamma}$ or ignoring it we end up with

$$|||e|||^2 \leq C \left(\|h\mathcal{R}(\hat{E}_h)\| + \|h^\alpha \mathcal{R}_\Gamma(\hat{E}_h)\|_{1/s, \Gamma_1 \cup \Gamma_2} + \mathcal{O}(h^\beta) \right) |||e|||. \quad (4.20)$$

This yields the desired result

$$|||e||| \leq C \left(\|h\mathcal{R}(\hat{E}_h)\| + \|h^\alpha \mathcal{R}_\Gamma(\hat{E}_h)\|_{1/s, \Gamma_1 \cup \Gamma_2} + \mathcal{O}(h^\beta) \right), \quad (4.21)$$

where assuming $\alpha \approx \beta \approx 1$, (4.21) is optimal. \square

4.3 A duality approach

In Theorem 2 we made a direct a priori error estimate. The a posteriori error estimates in Theorem 3 rely on bounds depending on the residual of the approximate solution, with no reference to the dual problem. There is yet another approach based on an adequate dual form of the original problem. This can be studied both in a priori as well as a posteriori regi. Below we give a version of the a priori estimate: Theorem 2 based on a dual problem formulation. This approach is quite similar to that of the proof of Theorem 2 and is included in here just in order to show the dual technique, as an alternative approach for the cases when establishing a reasonable convergence via Theorem 2 becomes too expensive. Here we assume that the dual problem has a sufficiently smooth solution in the weighted Sobolev space with a norm that naturally arises along the estimates. Now, we define the differential operator \mathcal{A} by

$$(\mathcal{A}\varphi, \mathbf{v}) = a(\varphi, \mathbf{v}), \quad \forall \varphi, \mathbf{v} \in W_h^E(\Omega),$$

and let $\mathcal{A} := \mathcal{A}_\Omega + \mathcal{A}_\Gamma$ where

$$\mathcal{A}_\Omega \varphi := s^2 \varepsilon(x) \varphi(x, s) - \Delta \varphi(x, s) - \nabla(\nabla \cdot (\varepsilon(x) - 1) \varphi(x, s)), \quad x \in \Omega$$

is a self adjoint operator, whereas

$$\mathcal{A}_\Gamma \varphi(x, s) := \partial_\nu(\varepsilon(x) \varphi(x, s)) + s \varphi(x, s), \quad x \in \Gamma_1 \cup \Gamma_2,$$

is non-self adjoint with the adjoint \mathcal{A}'_Γ given by

$$\mathcal{A}'_\Gamma \varphi(x, s) := -\partial_\nu(\varepsilon(x) \varphi(x, s)) + s \varphi(x, s), \quad x \in \Gamma_1 \cup \Gamma_2.$$

To proceed we consider the dual problem

$$\begin{cases} \mathcal{A}_\Omega \varphi(x, s) = e(x, s), & x \in \Omega \\ \mathcal{A}'_\Gamma \varphi(x, s) = -\partial_\nu(\varepsilon(x) e(x, s)) + s e(x, s), & x \in \Gamma_1 \cup \Gamma_2 \\ \partial_\nu \varphi(x, s) = 0, & x \in \Gamma_3. \end{cases} \quad (4.22)$$

Proposition 4.2 (Error estimate using dual problem). *Let $\varphi \in \mathbf{W}_E^2 := H_w^2(\Omega) \cap H_{1/s}^2(\Gamma)$ in the above duality formulation. Then, we have the following error estimate:*

$$\|e\| \leq h^2 \|\varphi\|_{H_w^2(\Omega)} + h^{3/2} \|\varphi\|_{H_{1/s}^2(\Gamma)},$$

Proof. For $\varphi \in \mathbf{W}_E^2$ and \mathbf{v} the nodal interpolant of φ in a finite element partition \mathcal{T}_h of the computational domain Ω , we have by a multiple use of Green's formula and a Galerkin

orthogonality relation that

$$\begin{aligned}
|||e|||^2 &= \|e\|_{s^2\varepsilon}^2 + \|\nabla e\|^2 + \|\nabla \cdot e\|_{\varepsilon^{-1}}^2 + \|e\|_{s,\Gamma_1 \cup \Gamma_2}^2 \\
&= (\mathcal{A}_\Omega \varphi, e) + (\mathcal{A}_\Gamma \varphi, e) \\
&= (\varphi, e)_{s^2\varepsilon} + (\nabla \varphi, \nabla e) + (\nabla \cdot ((\varepsilon - 1))\varphi, \nabla \cdot e) + \langle \varphi, e \rangle_{s,\Gamma_1 \cup \Gamma_2} \\
&= (\varphi - \mathbf{v}, e)_{s^2\varepsilon} + (\nabla(\varphi - \mathbf{v}), \nabla e) \\
&\quad + (\nabla \cdot ((\varepsilon - 1)\varphi - \mathbf{v}), \nabla \cdot e) + \langle \varphi - \mathbf{v}, e \rangle_{s,\Gamma_1 \cup \Gamma_2} \\
&\leq \|h^2 D^2 \varphi\|_{s^2\varepsilon} \|e\|_{s^2\varepsilon} + \|h D^2 \varphi\| \|\nabla e\| \\
&\quad + \|h D^2 \varphi\|_{\varepsilon^{-1}} \|\nabla \cdot e\|_{\varepsilon^{-1}} + \|h^{3/2} D^2 \varphi\|_{s,\Gamma_1 \cup \Gamma_2} \|e\|_{s,\Gamma_1 \cup \Gamma_2} \\
&\leq \left(\|h^2 D^2 \varphi\|_{s^2\varepsilon} + \|h D^2 \varphi\| + \|h D^2 \varphi\|_{\varepsilon^{-1}} + \|h^{3/2} D^2 \varphi\|_{s,\Gamma_1 \cup \Gamma_2} \right) |||e|||.
\end{aligned} \tag{4.23}$$

Thus

$$|||e||| \leq \|h\varphi\|_{H_w^2(\Omega)} + \|h^{3/2}\varphi\|_{H_s^2(\Gamma)},$$

which, is exactly the same estimate as in (4.6) and (4.21). Hence, the improved estimate (by $\mathcal{O}(h^{1/2})$) of order $\mathcal{O}(h^{3/2})$, due to the trace theorem is not helpful, due to the fact that the triple norm involves L_2 -norm of the gradient of the error and the final, optimal, estimate is of $\mathcal{O}(h)$. \square

4.4 Adaptivity algorithm

In this part we outline the adaptivity algorithm for the a posteriori error estimate given by (4.21). To this end we consider an *error tolerance* TOL and seek to construct a discrete scheme that would guarantee the error bound

$$|||e||| \leq \text{TOL}. \tag{4.24}$$

A concise adaptivity procedure is introduced as in the following steps

- I Given the dielectric permittivity function $\varepsilon(x)$, the initial data f_0 and the corresponding boundary conditions as in (2.4) and (2.5).
- II Consider a mesh size h , choose $\alpha \approx \beta \approx 1$ and compute the approximate initial data $f_{0,h}$ and the corresponding approximate solution \hat{E}_h , using the finite element scheme (3.10).
- III Use the definition of the residuals, viz. (4.8) and compute $\mathcal{R}(\hat{E}_h)$ and $\mathcal{R}_\Gamma(\hat{E}_h)$
- IV If

$$|||e||| \leq \left(\|h\mathcal{R}(\hat{E}_h)\| + \|h^\alpha \mathcal{R}_\Gamma(\hat{E}_h)\|_{1/s,\Gamma_1 \cup \Gamma_2} + \mathcal{O}(h^\beta) \right) \leq \text{TOL}, \tag{4.25}$$

(observe that we hide the constant C in TOL) then stop and accept the approximate solution \hat{E}_h . Otherwise, refine the mesh in the parts of the domain Ω and the boundary Γ where either or both of $\mathcal{R}(\hat{E}_h)$ and $\mathcal{R}_\Gamma(\hat{E}_h)$ are large and go to step II with this new mesh parameter.

5 Numerical examples

We perform numerical tests in the computational domain $\Omega = [0, 1] \times [0, 1]$, with $\Omega_1 := [0.25, 0.75] \times [0.25, 0.75]$. The source data (the right hand side) in the model problem (2.4) is chosen such that the function

$$\begin{aligned} E_1 &= \frac{1}{\varepsilon} 2\pi \sin^2 \pi x \cos \pi y \sin \pi y \frac{t^2}{2}, \\ E_2 &= -\frac{1}{\varepsilon} 2\pi \sin^2 \pi y \cos \pi x \sin \pi x \frac{t^2}{2} \end{aligned} \quad (5.1)$$

is the exact solution of this problem. After application of the Laplace transform (2.2) to (5.1) the exact solution of the transformed model problem (2.8) will be

$$\begin{aligned} E_1 &= \frac{2}{s^3 \varepsilon} \pi \sin^2 \pi x \cos \pi y \sin \pi y, \\ E_2 &= -\frac{2}{s^3 \varepsilon} \pi \sin^2 \pi y \cos \pi x \sin \pi x. \end{aligned} \quad (5.2)$$

In (5.1) the function ε is defined for an integer $m > 1$ as

$$\varepsilon(x, y) = \begin{cases} 1 + \sin^m \pi(2x - 0.5) \cdot \sin^m \pi(2y - 0.5) & \text{in } \Omega_1, \\ 1 & \text{in } \Omega_2 := \Omega \setminus \Omega_1. \end{cases} \quad (5.3)$$

The solution defined in (5.1) satisfies the homogeneous initial conditions. We chose homogeneous boundary conditions at the boundary $\Gamma = \partial\Omega$ of the computational domain Ω . Figure 2 shows the function ε for different values of m .

We discretize the computational domain $\Omega \times (0, T)$ denoting by $\mathcal{T}_{hl} = \{K\}$ a partition of the domain Ω into triangles K of sizes $h_l = 2^{-l}$, $l = 1, \dots, 6$. Numerical tests are performed for different $m = 2, \dots, 9$ in (5.3) and the relative errors are then measured in L_2 -norm and the H^1 -norms, respectively, which are computed as

$$e_l^1 = \frac{\|E - E_h\|_{L_2}}{\|E\|_{L_2}}, \quad (5.4)$$

$$e_l^2 = \frac{\|\nabla(E - E_h)\|_{L_2}}{\|\nabla E\|_{L_2}}, \quad (5.5)$$

where, as well as in the sequel

$$|E| := \sqrt{E_1^2 + E_2^2} \quad |E_h| := \sqrt{E_{1h}^2 + E_{2h}^2}. \quad (5.6)$$

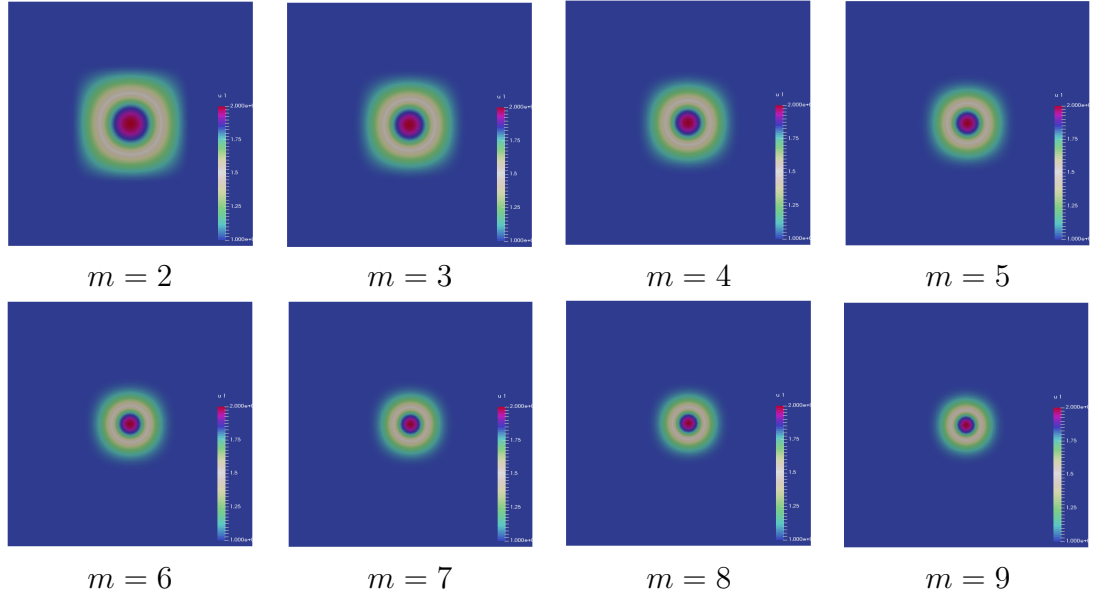


Figure 2: The function $\varepsilon(x, y)$ in the domain $\Omega = [0, 1] \times [0, 1]$ for different m in (5.3).

Figures 3-6 present convergence of P1 finite element numerical scheme for the function ε defined by (5.3) for $m = 2, \dots, 9$, see Figure 2 for this function. Tables 1-4 present convergence rates q_1, q_2 for $m = 2, 5, 7, 9$ which are computed accordingly

$$\begin{aligned}
 q_1 &= \frac{\log\left(\frac{el_h^1}{el_{2h}^1}\right)}{\log(0.5)}, \\
 q_2 &= \frac{\log\left(\frac{el_h^2}{el_{2h}^2}\right)}{\log(0.5)},
 \end{aligned} \tag{5.7}$$

where $el_h^{1,2}, el_{2h}^{1,2}$ are computed relative norms $el^{1,2}$ on the mesh \mathcal{T}_h with the mesh size h and $2h$, respectively. Similar convergence rates are obtained for $m = 3, 4, 5, 8$. Using these tables and figures we observe that our scheme behaves like a first order method for $H^1(\Omega)$ -

l	nel	nno	e_l^1	q_1	e_l^2	q_2
1	8	9	$2.71 \cdot 10^{-2}$		$8.60 \cdot 10^{-2}$	
2	32	25	$6.66 \cdot 10^{-3}$	2.02	$3.25 \cdot 10^{-2}$	1.40
3	128	81	$1.78 \cdot 10^{-3}$	1.90	$1.75 \cdot 10^{-2}$	$8.99 \cdot 10^{-1}$
4	512	289	$4.13 \cdot 10^{-4}$	2.11	$1.02 \cdot 10^{-2}$	$7.79 \cdot 10^{-1}$
5	2048	1089	$1.05 \cdot 10^{-4}$	1.97	$5.29 \cdot 10^{-3}$	$9.42 \cdot 10^{-1}$
6	8192	4225	$2.65 \cdot 10^{-5}$	1.99	$2.70 \cdot 10^{-3}$	$9.69 \cdot 10^{-1}$

Table 1: Relative errors in the L_2 -norm and in the H^1 -norm for mesh sizes $h_l = 2^{-l}$, $l = 1, \dots, 6$, for $m = 2$ in (5.3).

l	nel	nno	e_l^1	q_1	e_l^2	q_2
1	8	9	$2.35 \cdot 10^{-2}$		$1.20 \cdot 10^{-1}$	
2	32	25	$5.02 \cdot 10^{-3}$	2.22	$5.18 \cdot 10^{-2}$	1.21
3	128	81	$1.24 \cdot 10^{-3}$	2.02	$2.69 \cdot 10^{-2}$	$9.45 \cdot 10^{-1}$
4	512	289	$2.95 \cdot 10^{-4}$	2.07	$1.06 \cdot 10^{-2}$	1.34
5	2048	1089	$7.67 \cdot 10^{-5}$	1.94	$5.40 \cdot 10^{-3}$	$9.74 \cdot 10^{-1}$
6	8192	4225	$1.94 \cdot 10^{-5}$	1.99	$2.72 \cdot 10^{-3}$	$9.92 \cdot 10^{-1}$

Table 2: Relative errors in the L_2 -norm and in the H^1 -norm for mesh sizes $h_l = 2^{-l}$, $l = 1, \dots, 6$, for $m = 5$ in (5.3).

l	nel	nno	e_l^1	q_1	e_l^2	q_2
1	8	9	$2.28 \cdot 10^{-2}$		$1.15 \cdot 10^{-1}$	
2	32	25	$4.45 \cdot 10^{-3}$	2.36	$4.47 \cdot 10^{-2}$	1.35
3	128	81	$1.09 \cdot 10^{-3}$	2.03	$2.41 \cdot 10^{-2}$	$8.92 \cdot 10^{-1}$
4	512	289	$2.62 \cdot 10^{-4}$	2.05	$1.08 \cdot 10^{-2}$	1.16
5	2048	1089	$6.76 \cdot 10^{-5}$	1.95	$5.32 \cdot 10^{-3}$	1.01
6	8192	4225	$1.71 \cdot 10^{-5}$	1.98	$2.66 \cdot 10^{-3}$	$9.98 \cdot 10^{-1}$

Table 3: Relative errors in the L_2 -norm and in the H^1 -norm for mesh sizes $h_l = 2^{-l}$, $l = 1, \dots, 6$, for $m = 7$ in (5.3).

norm and second order method for $L^2(\Omega)$ -norm for all values of m . These results are all in good agreement with the analytic estimates derived in Theorems 1-3.

6 Conclusion

In this paper we consider the time harmonic Maxwell's equations obtained through Laplace transform applied to a time-dependent model problem with a certain variable, positive, di-

l	nel	nno	e_l^1	q_1	e_l^2	q_2
1	8	9	$1.73 \cdot 10^{-2}$		$7.29 \cdot 10^{-2}$	
2	32	25	$3.33 \cdot 10^{-3}$	2.38	$3.57 \cdot 10^{-2}$	1.03
3	128	81	$8.98 \cdot 10^{-4}$	1.89	$2.15 \cdot 10^{-2}$	$7.33 \cdot 10^{-1}$
4	512	289	$2.36 \cdot 10^{-4}$	1.93	$1.08 \cdot 10^{-2}$	$9.94 \cdot 10^{-1}$
5	2048	1089	$6.09 \cdot 10^{-5}$	1.96	$5.26 \cdot 10^{-3}$	1.04
6	8192	4225	$1.55 \cdot 10^{-5}$	1.98	$2.62 \cdot 10^{-3}$	1.00

Table 4: Relative errors in the L_2 -norm and in the H^1 -norm for mesh sizes $h_l = 2^{-l}$, $l = 1, \dots, 6$, for $m = 9$ in (5.3).

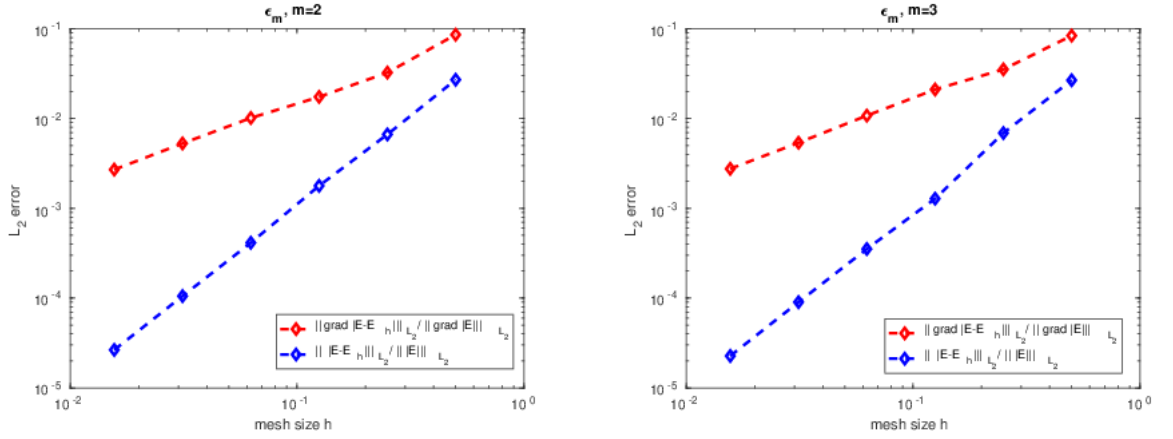


Figure 3: Relative errors for $m = 2$ (left) and $m = 3$ (right).

electric permittivity function $\varepsilon(x)$. Due to the varying nature of the dielectric permittivity function, we study the problem setting in a rectangular (cubic in $3d$) domain Ω split into an axi-parallel interior subdomain Ω_1 with varying $\varepsilon(x)$ and an outer domain $\Omega_2 := \Omega \setminus \Omega_1$, where $\varepsilon \equiv 0$. Thus, Ω_1 and Ω_2 are two disjoint open sets with a, partially, common boundary (see Fig. 1). In multiscale setting they may be considered as the domains of fine and coarse numerical resolutions. We construct a $P1$ stabilized finite element approximations for this problem and prove its consistency and well-posedness. As for the accuracy of the constructed numerical scheme we derive, optimal, a priori and a posteriori error bounds, in some, gradient dependent, weighted energy norms.

The optimality is conformed both in forward and dual constructions which yield the same convergence rates. The involved weight function appears in different forms and combines the dielectric permittivity and the Laplace transformation variable. We have implemented several numerical examples that validate the robustness of the theoretical studies.

This problem is of vital importance in solving the *Coefficient Inverse Problems* (CIPs)

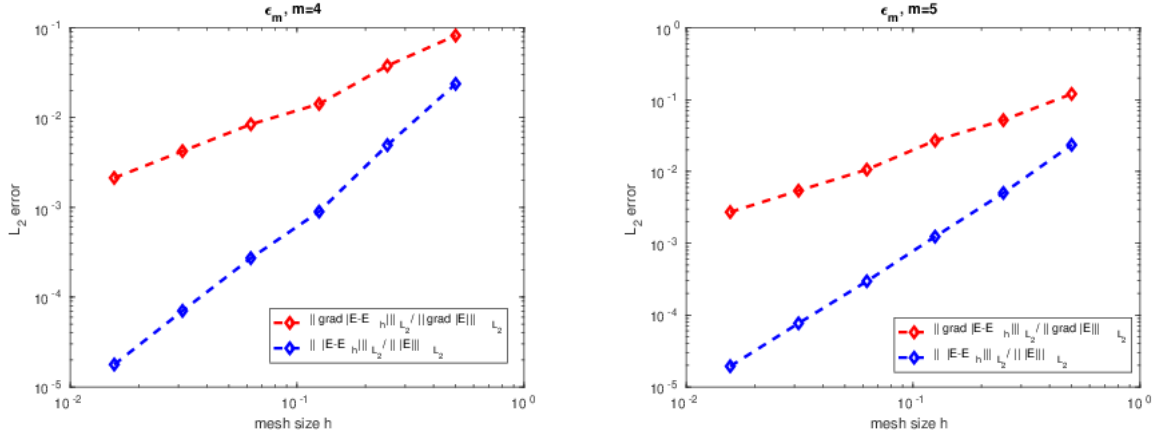


Figure 4: Relative errors for $m = 4$ (left) and $m = 5$ (right).

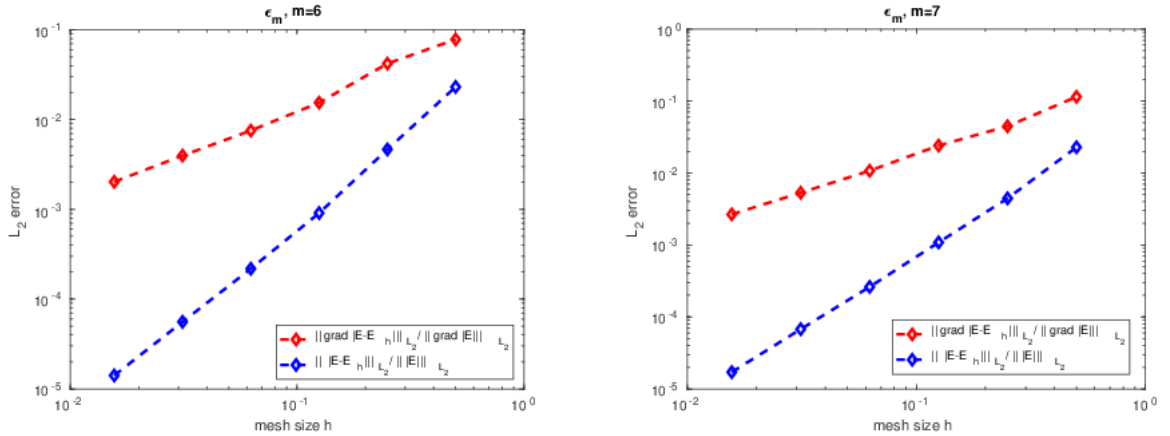


Figure 5: Relative errors for $m = 6$ (left) and $m = 7$ (right).

with several applications ranging from medical physics (radiation therapy) to micro turbines, computer chips, devices in fusion energy studies and so on. For the study of a corresponding time-dependent problem we refer to, e.g., [4]. In many application, to determine a reliable dielectric permittivity function, the time-dependent Maxwell's equations are required in the entire space \mathbb{R}^3 , see, e.g., [5, 6, 7, 10, 32, 33]. In present study, however, it is more efficient to consider Maxwell's equations in bounded domain, with constant dielectric permittivity function in a neighborhood of the boundary of the computational domain. The P1 finite element scheme of [2] is used for solution of different CIPs to determine the dielectric permittivity function in non-conductive media for time-dependent Maxwell's equations using simulated and experimentally generated data, see, e.g., [1, 3, 5, 6, 7, 10, 32, 33].

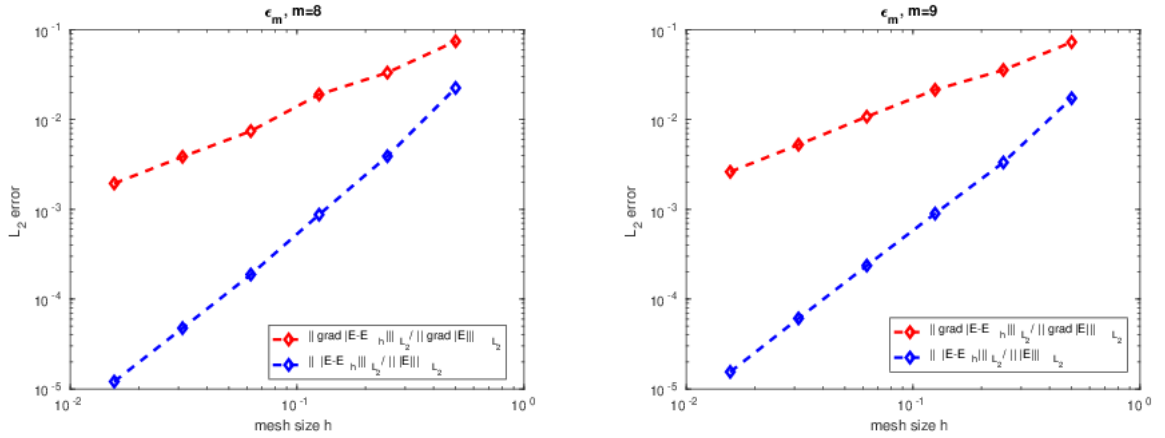


Figure 6: Relative errors for $m = 8$ (left) and $m = 9$ (right).

Acknowledgment: The research of both authors is supported by the Swedish Research Council grant VR 2018-03661. The first author acknowledges the support of the VR grant DREAM. ■

References

- [1] L. Beilina, Application of the finite element method in a quantitative imaging technique, *J. Comput. Methods Sci. Eng.*, IOS Press, 16(4), 755-771, 2016. DOI 10.3233/JCM-160689.
- [2] L. Beilina, Energy estimates and numerical verification of the stabilized Domain Decomposition Finite Element/Finite Difference approach for time-dependent Maxwell's system, *Cent. Eur. J. Math.*, 11, 702-733, 2013. DOI: 10.2478/s11533-013-0202-3.
- [3] L. Beilina, M. Cristofol and K. Niinimäki, Optimization approach for the simultaneous reconstruction of the dielectric permittivity and magnetic permeability functions from limited observations, *Inverse Problems and Imaging*, 9 (1), 1-25, 2015.
- [4] L. Beilina, V. Ruas, An explicit P1 finite element scheme for Maxwell's equations with constant permittivity in a boundary neighborhood, arXiv:1808.10720.
- [5] L. Beilina and M. V. Klibanov, *Approximate global convergence and adaptivity for Coefficient Inverse Problems*, Springer, New York, 2012.
- [6] L. Beilina, N. T. Th'anh, M. Klibanov, and J. B. Malmberg, Reconstruction of shapes and refractive indices from blind backscattering experimental data using the adaptivity, *Inverse Problems*, 30, 105007, 2014.

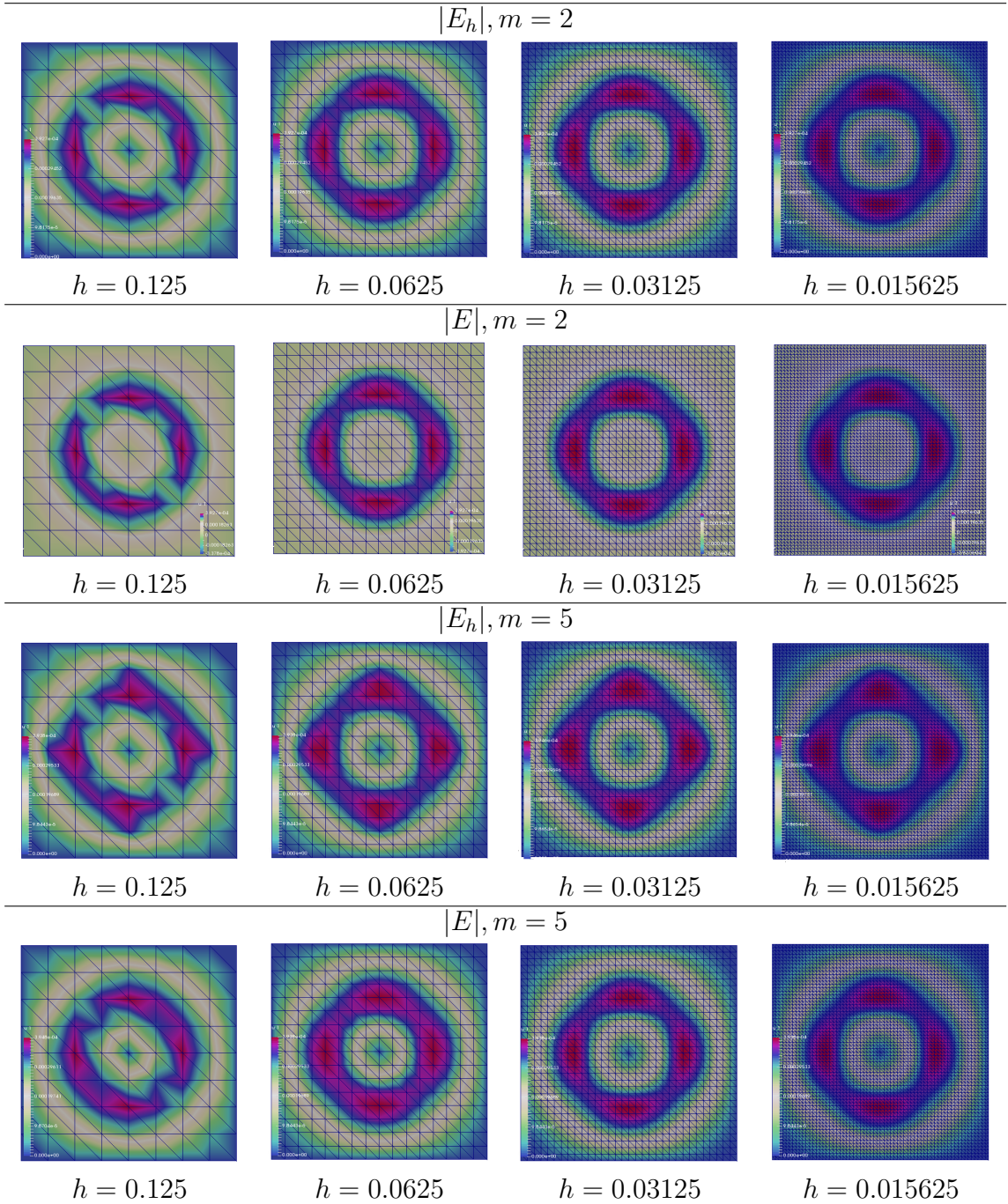


Figure 7: *Computed vs. exact solution for different meshes taking $m = 2$ and $m = 5$ in (5.3).*

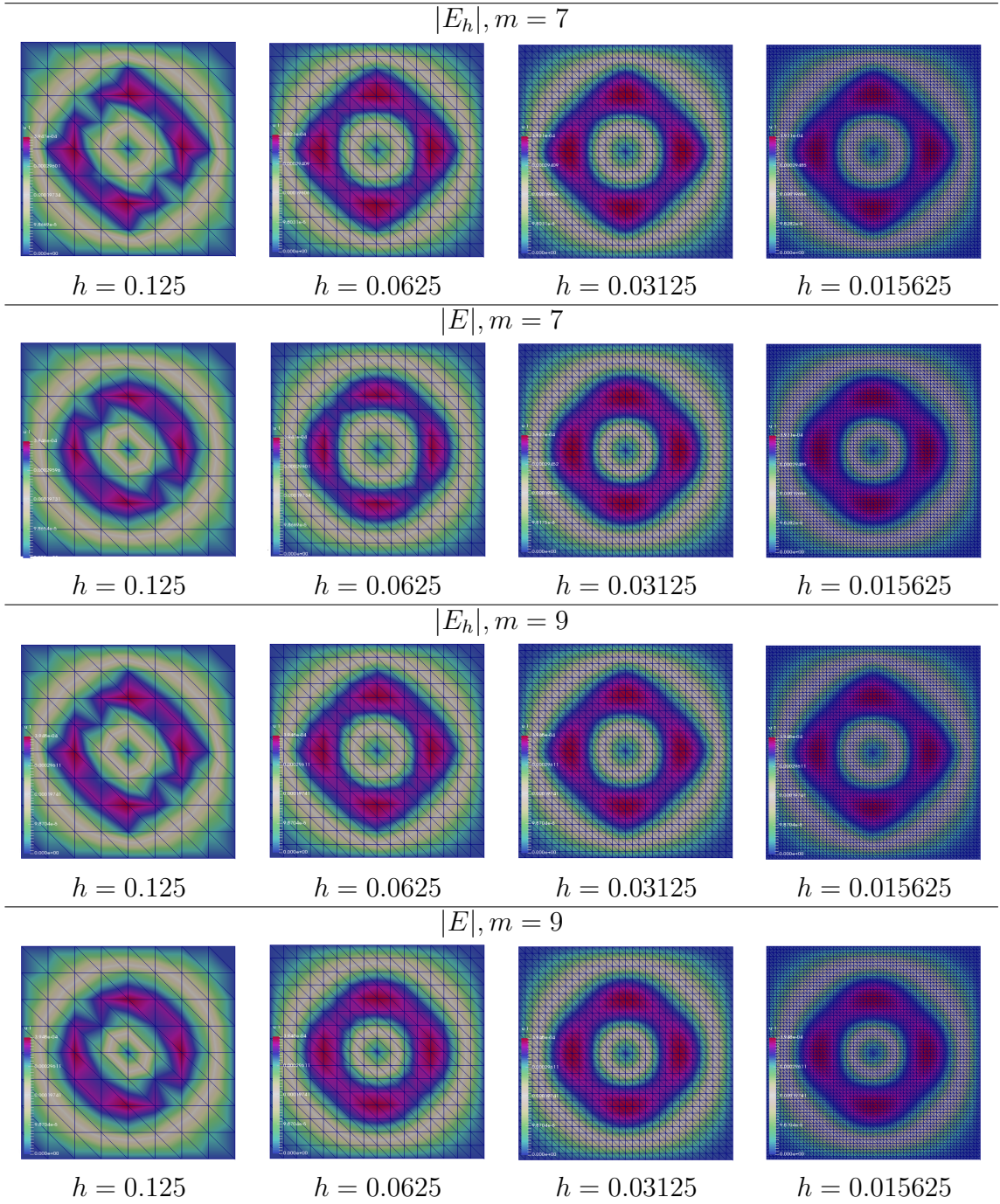


Figure 8: *Computed vs. exact solution for different meshes taking $m = 2$ and $m = 5$ in (5.3).*

- [7] L. Beilina, N. T. Th'anh, M.V. Klibanov and J. B. Malmberg, Globally convergent and adaptive finite element methods in imaging of buried objects from experimental backscattering radar measurements, *Journal of Computational and Applied Mathematics, Elsevier*, DOI: 10.1016/j.cam.2014.11.055, 2015.
- [8] M. Bellassoued, M. Cristofol, and E. Soccorsi, Inverse boundary value problem for the dynamical heterogeneous Maxwell's system, *Inverse Problems*, 28, 095009(188pp), 2012.
- [9] S. C. Brenner and L. R. Scott, *The Mathematical Theory of Finite Element Methods*, Springer-Verlag, Berlin, 1994.
- [10] J. Bondestam Malmberg, L. Beilina, An Adaptive Finite Element Method in Quantitative Reconstruction of Small Inclusions from Limited Observations, *Appl. Math. Inf. Sci.*, 12(1), 1-19, 2018.
- [11] V. A. Burov, S. A. Morozov, and O. D. Romyantseva, Reconstruction of fine-scale structure of acoustical scatterers on large-scale contrast background, *Acoustical Imaging*, 26 231-238, 2002.
- [12] Y. Chen, Inverse scattering via Heisenberg uncertainty principle, *Inverse Problems*, 13, 253-282, 1997.
- [13] G. C. Cohen, *Higher Order Numerical Methods for Transient Wave Equations*, Springer-Verlag, Berlin, 2002.
- [14] A. E. Bulyshev, A. E. Souvorov, S. Y. Semenov, V. G. Posukh and Y. E. Sizov, Three-dimensional vector microwave tomography: theory and computational experiments, *Inverse Problems*, 20(4), pp.1239-1259, 2004.
- [15] A. Elmkies and P. Joly, Finite elements and mass lumping for Maxwell's equations: the 2D case. *Numerical Analysis*, C. R. Acad.Sci.Paris, 324, pp. 1287–1293, 1997.
- [16] H. W. Engl, M. Hanke, and A. Neubauer, *Regularization of Inverse Problems*, Kluwer Academic Publishers, Dordrecht, The Netherlands, 1996.
- [17] B. Engquist and A. Majda, Absorbing boundary conditions for the numerical simulation of waves, *Math. Comp.*, 31, 629-651, 1977.
- [18] B. Jiang, *The Least-Squares Finite Element Method. Theory and Applications in Computational Fluid Dynamics and Electromagnetics*, Springer-Verlag, Heidelberg, 1998.
- [19] B. Jiang, J. Wu and L. A. Povinelli, The origin of spurious solutions in computational electromagnetics, *Journal of Computational Physics*, 125, 104-123, 1996.
- [20] J. Jin, *The finite element method in electromagnetics*, Wiley, 1993.
- [21] P. Joly, Variational methods for time-dependent wave propagation problems, *Lecture Notes in Computational Science and Engineering*, Springer, 2003.

- [22] G. Chavent, *Nonlinear Least Squares for Inverse Problems. Theoretical Foundations and Step-by-Step Guide for Applications*, Springer, New York, 2009.
- [23] W.T. Joines, Y. Zhang, C. Li, and R. L. Jirtle, The measured electrical properties of normal and malignant human tissues from 50 to 900 MHz', *Med. Phys.*, 21 (4), 547-550, 1994.
- [24] N. Joachimowicz, C. Pichot and J. P. Hugonin, Inverse scattering: and iterative numerical method for electromagnetic imaging, *IEEE Trans. Antennas Propag.*, 39 (12), 1742-1753, 1991.
- [25] P. B. Monk, *Finite Element methods for Maxwell's equations*, Oxford University Press, 2003.
- [26] P. B. Monk and A. K. Parrott, A dispersion analysis of finite element methods for Maxwell's equations, *SIAM J.Sci.Comput.*, 15, 916-937, 1994.
- [27] C. D. Munz, P. Omnes, R. Schneider, E. Sonnendrucker and U. Voss, Divergence correction techniques for Maxwell Solvers based on a hyperbolic model, *Journal of Computational Physics*, 161, 484-511, 2000.
- [28] J.-C. Nédélec, Mixed finite elements in R3, *Numerische Mathematik*, 35, 315-341, 1980.
- [29] K. D. Paulsen, D. R. Lynch, Elimination of vector parasites in Finite Element Maxwell solutions, *IEEE Transactions on Microwave Theory Technologies*, 39, 395 –404, 1991.
- [30] O.Pironneau, *Optimal Shape Design for Elliptic Systems*, Springer-Verlag, Berlin, 1984.
- [31] Portable, Extensible Toolkit for Scientific Computation PETSc at <http://www.mcs.anl.gov/petsc/>
- [32] N. T. Thánh, L. Beilina, M. V. Klibanov, and M. A. Fiddy, Reconstruction of the refractive index from experimental backscattering data using a globally convergent inverse method, *SIAMJ. Sci. Comput.*, 36, B273-B293, 2014.
- [33] N. T. Thánh, L. Beilina, M. V. Klibanov, M. A. Fiddy, Imaging of Buried Objects from Experimental Backscattering Time-Dependent Measurements using a Globally Convergent Inverse Algorithm, *SIAM Journal on Imaging Sciences*, 8(1), 757-786, 2015.
- [34] Software package WavES at <http://www.waves24.com/>